

# RADIOMETRIC BLOCK-ADJUSTMENT OF SATELLITE IMAGES REFERENCE3D® PRODUCTION LINE IMPROVEMENT

L. Falala<sup>a</sup>, R. Gachet<sup>a</sup>, L. Cunin<sup>a</sup>

<sup>a</sup>IGN, Institut Géographique National, 6 Avenue de l'Europe, 31520 Ramonville,  
France - (laurent.falala, roland.gachet, laurent.cunin)@ign.fr

**Commission, WG IV/3**

**KEY WORDS:** SPOT, Radiometry, Mosaic, Block, Multitemporal, Orthoimage

## **ABSTRACT:**

One layer of global geographic database Reference3D® is an image mosaic (5m resolution) made exclusively from panchromatic SPOT5-HRS images. In order to improve Reference3D® production line, in particular SPOT5 HRS images mosaicking step, a new strategy of radiometric block adjustment of satellite images was developed, implemented and tested at French mapping agency IGN. By analogy with “geometric” block adjustment, we developed an iterative algorithm, adapted to Reference3D datasets (many overlapping images covering a wide area), that calculates for each image a polynomial model to apply to its radiometry. These polynomials are found by least-square resolution of a global linear system. Among many tests conducted to try different parameters and validate the process, we present here results of a test case over Algeria (9 not too cloudy images taken in less than 3 months) and another more difficult over Tasmania (11 very cloudy images taken in 4 years). In both cases, radiometric differences between images were dramatically reduced. Reference3D contains also a DEM obtained by merging overlapping DEMs (calculated by automatic image matching of SPOT5-HRS stereo-pairs). Radiometric block adjustment methodology can be easily adapted for DEMs tilting, a preliminary step before merging. So, thanks to these new processes, previously manual tasks in reference3D® production line are now mostly automatic.

## **1. CONTEXT**

### **1.1 Reference3D® database**

Reference3D® is a global geographic database produced by Spot Image and French mapping agency IGN. It contains three layers of information:

- DTED2 Digital Elevation Models (DEM with pixel size at 1”),
- 5m panchromatic ortho-images,
- Quality and traceability metadata (including water and cloud masks).

Reference3D® is made exclusively from SPOT5-HRS stereo-pairs with the following production line:

- Block adjustment of large sets of HRS stereo-pairs,
- DEM generation by automatic image matching of stereo-pairs,
- Orthorectification of every HRS scene with previously generated DEM,
- Image mosaicking and DEM merging,
- Quality metadata editing, tiling and packaging.

Annual production rate reaches 7 million km<sup>2</sup> in 2007 but studies are conducted to improve productivity, especially to automate previously manual tasks. For this purpose, a new algorithm of automatic radiometric block-adjustment was developed, implemented and tested on real Reference3D® datasets. It performs automatic radiometric adjustment and helps to build a cloud mask, which improve image mosaicking and metadata editing steps. It can be used also to tilt DEM, which may be necessary for DEM merging step.

### **1.2 Radiometric adjustment techniques**

Radiometric block adjustment consists in modifying radiometry of each image of a block in order to reduce radiometric difference between images and create a more visually pleasing and almost seamless mosaic. Various methodologies exist to complete this task, each tailored to a particular context.

Radiometric adjustment, based on physical modelling of solar illumination, has been developed for mosaics of cloud-free, mono-date and multispectral aerial images (Martinoty 2005). But Reference3D input images are multi-temporal and distributed throughout the world, making any physical modelling too complex if not impossible.

On the other hand, image harmonization and cloud detection techniques exist for low-resolution satellite images with many spectral bands, like NASA cloud masking algorithm on MODIS images (Ackerman, 1998). But such methods can't be used on panchromatic SPOT5-HRS images containing only one spectral band.

## **2. METHODOLOGY**

### **2.1 Introduction**

By analogy with “geometric” block adjustment, we developed a radiometric adjustment methodology adapted to Reference3D datasets made of many overlapping images covering a wide area. This non-physical iterative algorithm calculates a polynomial model for each image of the block, by least-square resolution of a global linear system. At the end of this process, radiometry of any pixel (column, row) of a given image  $I$  is modified as follows (eq. 1):

$$FinalRadio_{imgI}(col,row) = [1 + P_I(col,row)] \cdot IniRadio_{imgI}(col,row) + Q_I(col,row) \quad (1)$$

$$\begin{cases} P_{imgI}(col,row) \cdot IniRadio_{imgI}(col,row) / \sigma_{PI} = 0 \\ Q_{imgI}(col,row) / \sigma_{QI} = 0 \end{cases} \quad (3)$$

where  $P_I$  and  $Q_I$  are polynomials of varying degrees. With constant polynomials, this formula becomes a simple look-up table (LUT) and with polynomials of degree one and above, image radiometry correction according to pixel location.

## 2.2 Building a grid of radiometric values

First step of radiometric block adjustment consists in building a regular grid of radiometric values, extracted from the block of overlapping images to harmonize. Each useful grid node contains one or several radiometric values, depending of how many images it covers. These values are calculated by interpolation in initial image, sub-sampled at a given resolution. A radiometric initial threshold is applied so that too bright points, supposed to be part of clouds, are invalidated. A global mask, for example a water mask, can also be used to reduce the number of invalid points. Finally, these radiometric values are going to fuel a single large equation system.

## 2.3 Fuelling the system with observation equations

Observation equations are set up to equalize final radiometry of images on overlapping areas. They are written for each grid node containing at least two values, as in the following example for a node over images 1 and 2 (eq. 2).

$$\frac{FinalRadio_{img1}(col1,row1)}{\sigma_{Obs}} = \frac{FinalRadio_{img2}(col2,row2)}{\sigma_{Obs}}$$

$$\Leftrightarrow \frac{\left[ \begin{array}{l} [1 + P_{img1}(col1,row1)] \cdot IniRadio_{img1}(col1,row1) \\ + Q_{img1}(col1,row1) \end{array} \right]}{\sigma_{Obs}} = \frac{\left[ \begin{array}{l} [1 + P_{img2}(col2,row2)] \cdot IniRadio_{img2}(col2,row2) \\ + Q_{img2}(col2,row2) \end{array} \right]}{\sigma_{Obs}} \quad (2)$$

where:

- $IniRadio_{img1}(col1,row1)$  is the radiometric value extracted from image1 at (col1,row1) position,
- $IniRadio_{img2}(col2,row2)$  is the radiometric value extracted from image2 at (col2,row2) position,
- $\sigma_{Obs}$  is used to weight the equation

With only observation equations, this system has a set of obvious solutions:  $P=-1$  and  $Q=constant$  value for any image. All images become uniform and information is totally lost. That is why we have to add constraint equations to the system to avoid this unacceptable solution.

## 2.4 Adding constraint equations to the system

**2.4.1 Constraints on initial radiometry invariance:** These constraint equations are set up to maintain final radiometry same as initial radiometry for all valid grid nodes, those on overlapping areas but also those covering only one image. In practice, we write two equations for a given image I (eq. 3):

where:

- $IniRadio_{imgI}(col,row)$  is the radiometric value extracted from image I at (col,row) position,
- $\sigma_{PI}$  and  $\sigma_{QI}$  are used to weight equations. These values are set image by image.

Relative weighting of constraint equations compared to observation equations lets image radiometry to change more or less. With a very constrained system, final radiometry will be very close to initial one. On the contrary, radiometry can change a lot with a less constrained system, with the risk of reducing dynamic of images due to influence of observation equations. As weighting can be done image by image, we have here a way to fix radiometry of an image by giving very low values to its  $\sigma_{PI}$  and  $\sigma_{QI}$ .

## 2.4.2 Constraints on global average invariance by image:

These constraints are used to modify global radiometric average value of each image. Precisely, they try to make final radiometry average of all valid grid points concerning an image equal to valid initial average of the whole grid. We write as much equations (eq. 4) as there are images in the dataset.

$$\frac{FinalRadio\_Average\_imgI}{\sigma_{Av\ imgI}} = \frac{InitialRadio\_Average\_Grid}{\sigma_{Av\ imgI}} \quad (4)$$

Weighting can be done image by image to control how average radiometry of an image gets closer to global average of the dataset.

**2.4.3 Constraints on global average invariance:** As an alternative to global constraints by image defined in the previous paragraph, we can just add one single global constraint on average invariance. We write one equation (eq. 5) that tries to make final radiometry average of all valid grid points equal to valid initial average.

$$\frac{FinalRadio\_Average\_Grid}{\sigma_{Av\ Grid}} = \frac{InitialRadio\_Average\_Grid}{\sigma_{Av\ Grid}} \quad (5)$$

Weighting is global and helps to control average radiometry of the whole dataset.

## 2.5 System solving and validity updating

All equations are weighted differently in order to favour observations or a type of constraints. Weighting can also be tuned image per image and some images can be considered as invariant. Polynomial coefficients for each image are calculated globally by least-square resolution of this linear system composed by observation and constraints equations.

Once the system is solved, validity of all grid nodes is updated. A node covering only one image is always considered as valid whereas a node over at least two images can be invalidated if its final radiometries are too different. A previously invalidated

grid node can be re-validated as well. The full process may be re-iterated as needed.

After the last iteration, each image has its own radiometric polynomial model (eq. 1) and cloud masks can be extracted from invalid points.

### 3. IMPLEMENTATION AND TESTS

#### 3.1 Implementation

This algorithm has been implemented in GeoView Software, a photogrammetry and remote sensing suite developed in-house at IGN-France. We focused on SPOT5-HRS images but his module works also with any type of ortho-images or raw images with location modelling. It also works with multispectral images. In this case, each channel is radiometrically adjusted independently.

#### 3.2 Test case over Algeria

**3.2.1 Dataset overview:** 9 SPOT5 HRS stereo-pairs covering a part of Algerian territory are used to test previously described process of radiometric block adjustment. It is a medium size dataset that can be considered as quite easy and favourable because:

- There are large overlapping areas between images (20-25%),
- Interval between first image taken on 09/08/2002 and last image taken on 26/10/2002 is very short, less than 3 months,
- Very few clouds are present in images.

Radiometric adjustment is done on ortho-images calculated from back images of HRS stereo-pairs. These ortho-images are very large, up to 57474 columns by 115981 rows, their pixel size is 5m and the whole dataset covers 6° of longitude by 8° of latitude (530 km \* 970 km). A global mask over Mediterranean Sea is added.

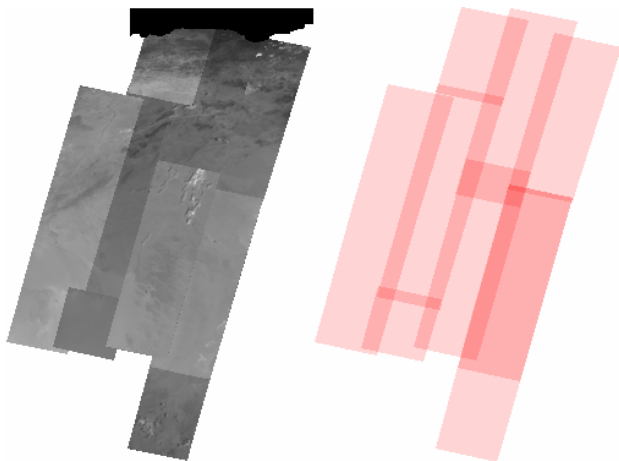


Figure 1. SPOT5 HRS images over Algeria - Dataset overview

**3.2.2 Influence of parameters:** Radiometry is extracted every 1000 m from sub-sampled images at 100m. To speed up the process, images are saved in a pyramidal format so that radiometry is interpolated directly in the right pyramid level. A grid node is ignored if it covers global mask and invalidated if its calculated radiometry is superior to initial threshold (180). Here, we get 412143 valid radiometric values to set up the global equation system. Degrees of polynomials P and Q are set to 1, so radiometric model for a given image I is as follows (eq. 6):

$$FinalRad(col,row) = [1 + a_1 \cdot col + b_1 \cdot row + c_1] \cdot InitialRad(col,row) + [d_1 \cdot col + e_1 \cdot row + f_1] \quad (6)$$

There are 6 unknown values by image, 54 for the whole system that is therefore very redundant. Role of every parameter has been studied but let's focus on punctual constraints influence. With  $\sigma_P = \sigma_Q = \sigma$  the value used to weight punctual constraint equations (eq. 3), Table 1 and Figures 2, 3 show huge influence of these punctual constraints on final radiometry. With  $\sigma=10$ , RMS of radiometric differences on overlapping area drop from 26.5 numerical counts to 4.4, final mosaic is seamless and image dynamic is kept. Whereas, with  $\sigma=0.1$  and  $\sigma=1$ , the system is too rigid, final radiometry close to initial one and seams remain visible. With  $\sigma=100$ , final image dynamic is very poor. Standard deviation of radiometric values stored in the grid drops to 3.3, too much information has been lost.

	% valid nodes	Grid average radiometry	Grid std dev	Residual RMS
Initial	99.1	100.2	25.9	26.5
$\sigma=0.1$	98.5	100.2	17.2	13.5
$\sigma=1$	98.1	100.2	14.7	7.8
$\sigma=10$	93.8	100.2	11.1	4.4
$\sigma=100$	93.8	100.2	3.3	0.5

Table 1. Influence of punctual constraints

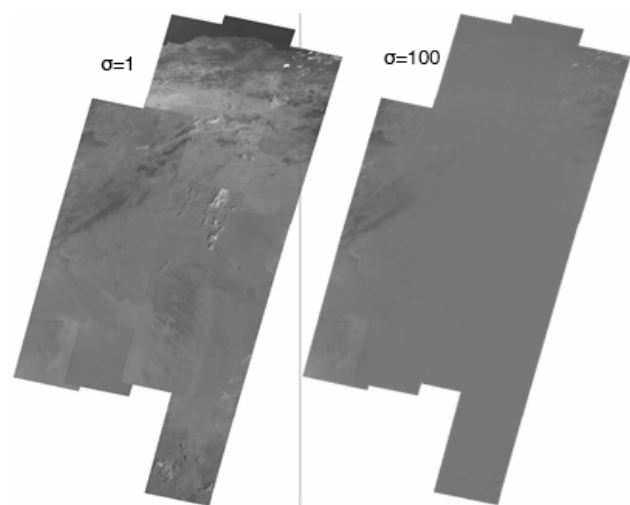


Figure 2. Influence of punctual constraints on final radiometry

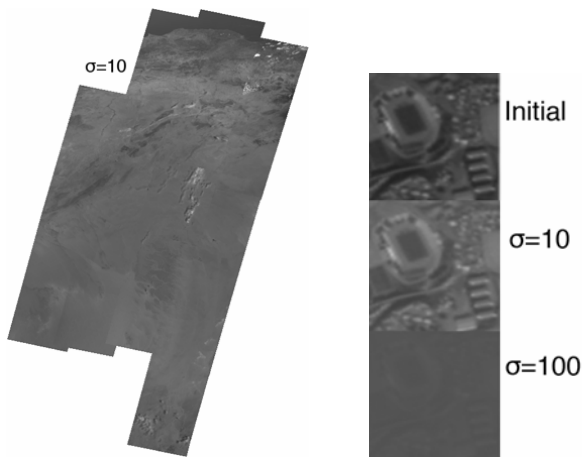


Figure 3. Influence of punctual constraints on final radiometry

### 3.3 Test case over Tasmania

The process has been tested on Tasmania Island, southeast of Australia. Due to oceanic climate, input data is very heterogeneous. Eleven very cloudy SPOT5-HRS segments taken from 2004 to 2007 in winter (July) as in summer (January) were required to cover nearly 70000 km<sup>2</sup>. With one point every kilometre, an initial water mask and two iterations, results are promising. Degree 1 polynomials make globally well-adjusted

images (Fig. 4). RMS of radiometric differences on overlapping area drops from 62 to 14. And consequently, seams between images are less visible if not invisible (Fig. 5).

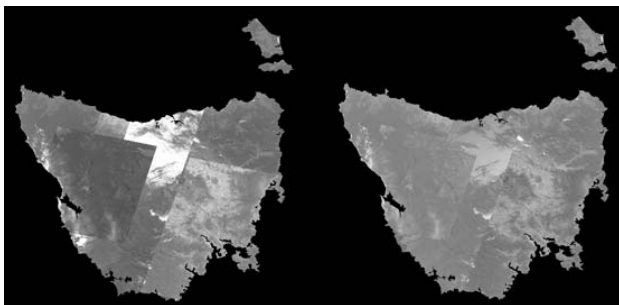


Figure 4. Initial and final radiometries - Tasmania

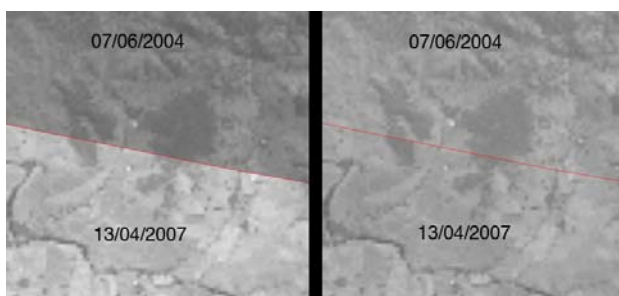


Figure 5. initial and final limit between 2 images - Tasmania

For each image, a cloud mask is created automatically from invalid grid nodes (Fig. 6). These masks have proved to be very useful for mosaicking step.

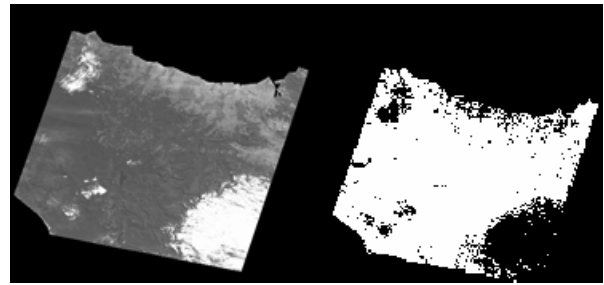


Figure 6. Image and cloud mask - Tasmania

## 4. APPLICATION TO DEM TILTING

Reference3D DEM is obtained by merging overlapping DEMs, calculated by automatic image matching of SPOT5-HRS stereo-pairs. But residual errors in “geometric” block adjustment result in small altimetric discontinuities between DEMs so tilting them is necessary before merging step. Radiometric block adjustment methodology can be adapted easily for DEM tilting. Image radiometry is simply replaced by DEM altitude and polynomial model applied to altitude is as follows (eq.7):

$$FinalAlt(col,row) = InitialAlt(col,row) + Q(col,row) \quad (7)$$

where:

- InitialAlti is initial DEM altitude for pixel (col,row)
- FinalAlti is calculated altitude for pixel (col,row)
- Q is a polynomial limited to degree 1.

Multiplier polynomial P, present for radiometric block adjustment, is not used for DEM tilting. Addition to initial altitude is the only permitted operation, multiplication is forbidden.

## 5. PERSPECTIVES

Radiometric block-adjustment strategy described in this article has been validated on medium-size datasets. Previously manual tasks like radiometric adjustment or DEM tilting are now mostly automatic and give good results. But, many studies could be conducted to improve this algorithm, in particular concerning system constraints on standard deviation invariance to have a better control of image dynamic. And practically, this functionality has yet to be transferred to Reference3D mass production, typically from Tasmania dataset to Australia dataset.

## REFERENCES

- Ackerman, S.A., Strabala, K. I., Menzel, P. W.P., Frey, R.A., Moeller, C.C. and Gumley, L.E., 1998: Discriminating clear sky from clouds with MODIS, *Journal of Geophysical Research*, 103(D24):32,141-32,157.
- Caprioli, M., Figorito, B. and Tarantino, E., 2006. Radiometric Normalization of Landsat Etm+ Data for Multitemporal Analysis, *ISPRS Proceedings “From pixels to processes”*, Enschede (NL).

- Furby, S.L., Campbell, N.A., 2001. Calibrating images from different dates to "like value" digital counts, *Remote Sensing of Environment*, 77: 186-196.
- Hall, F.G., Strebel, D.E., Nickeson, J.E. and Goetz, S.J., 1991. Radiometric rectification: toward a common radiometric response among multirate, multisensor images, *Remote Sensing of Environment*, 35: 11-27.
- Martinoty, G., 2005. Reconnaissance de matériaux sur des images aériennes en multirecouvrement, par identification de fonctions de réflectances bidirectionnelles. *Thèse de doctorat de l'Université Paris 7*.
- Paolini, L., Grings, F., Sobrino, J.A., Jiménez Muñoz, J.C. and Karszenbaum, H., 2006. Radiometric correction effects in Landsat multi-date/multi-sensor change detection studies, *International Journal of Remote Sensing*, 27(4): 685-704.
- Petit, M., Faure, J.F., Girres, J.F., Ose, K., Durieux, L., Huynh, F., Lasselin, D., Deshayes, M. and Stach, N., 2007. A first global spot mosaic of French Guiana in the Framework of Kyoto protocol by direct receiving station SEAS-Guyane facility. Colloque international ForestSat'07. Montpellier (France).
- Tucker, C.J., Grant, D.M. and Dykstra, J.D., 2004. NASA's global orthorectified Landsat data set, *Photogrammetric Engineering and Remote Sensing*, 70(3): 313-322.
- Xandri, R., Pérez, F., Palà, V., Arbiol, R., 2005. Automatic Generation of Seamless Mosaics over Extensive Areas from High Resolution Imagery. World Multi-Conference on Systemics, Cybernetics and Informatics (WMSCI). Orlando, USA.

